

# Engineering a CRISPR Interference System To Repress a Class 1 Integron in *Escherichia coli*

Qingyang Li,<sup>a</sup> Peng Zhao,<sup>b</sup> Lili Li,<sup>c</sup>  Haifeng Zhao,<sup>a</sup> Lei Shi,<sup>c</sup>  Pingfang Tian<sup>b</sup>

<sup>a</sup>School of Food Science and Engineering, South China University of Technology, Guangzhou, China

<sup>b</sup>College of Life Science and Technology, Beijing University of Chemical Technology, Beijing, China

<sup>c</sup>Institute of Food Safety and Nutrition, Jinan University, Guangzhou, China

**ABSTRACT** Microbial multidrug resistance (MDR) poses a huge threat to human health. Bacterial acquisition of MDR relies primarily on class 1 integron-involved horizontal gene transfer (HGT) of antibiotic resistance genes (ARGs). To date, no strategies other than the use of antibiotics can efficiently cope with MDR. Here, we report that an engineered CRISPR interference (CRISPRi) system can markedly reduce MDR by blocking a class 1 integron in *Escherichia coli*. Using CRISPRi to block plasmid R388 class 1 integron, *E. coli* recombinants showed halted growth upon exposure to relevant antibiotics. A microplate alamarBlue assay showed that both subgenomic RNAs (sgRNAs) R3 and R6 led to 8- and 32-fold decreases in half-maximal inhibitory concentrations (IC<sub>50</sub>) for trimethoprim and sulfamethoxazole, respectively. Reverse transcription and quantitative PCR (RT-qPCR) revealed that the strain employing sgRNA R6 exhibited 97% and 84% decreases in the transcriptional levels of the *dfrB2* cassette and *sul1*, two typical ARGs, respectively. RT-qPCR analysis also demonstrated that the strain recruiting sgRNA R3 showed a 96% decrease in the transcriptional level of *int11*, and a conjugation assay revealed a 1,000-fold decrease in HGT rates of ARGs. Overall, the sgRNA R3 targeting the 31 bp downstream of the Pc promoter on the *int11* nontemplate strand outperformed other sgRNAs in reducing integron activity. Furthermore, this CRISPRi system is reversible, genetically stable, and titratable by varying the concentration of the inducer. To our knowledge, this is the first report on exploiting a CRISPRi system to reduce the class 1 integron in *E. coli*. This study provides valuable insights for future development of CRISPRi-based antimicrobial agents and cellular therapy to suppress MDR.

**KEYWORDS** CRISPR interference, class 1 integron, horizontal gene transfer, antibiotic resistance gene, multidrug resistance

Recent years have witnessed the severe threat of antibiotic-resistant pathogens (ARPs) to human health (1). In the United States, approximately 2 million patients each year are infected with ARPs, resulting in at least 23,000 fatalities, and this situation is getting worse (2). Antibiotics have been extensively harnessed to combat pathogen infections. However, overuse of them accelerates the evolution of microbial multidrug resistance (MDR), and this situation necessitates combinatorial use of antibiotics (1, 3). MDR is largely attributed to horizontal gene transfer (HGT) of antibiotic resistance genes (ARGs), and HGT is typically accomplished by mobile genetic elements (MGEs) through transformation, conjugation, and transduction (3, 4). Among all types of MGEs, mobile integrons (MIs) are commonly found in clinical settings and other circumstances (5–9) and played a crucial role in the early rise of MDR among clinically relevant bacteria in the 1960s (5). Indeed, increasing evidence has shown that the transmission of ARGs among Gram-negative pathogens is frequently brought by the MI-involved HGT of ARGs (9–11).

**Citation** Li Q, Zhao P, Li L, Zhao H, Shi L, Tian P. 2020. Engineering a CRISPR interference system to repress a class 1 integron in *Escherichia coli*. *Antimicrob Agents Chemother* 64:e01789-19. <https://doi.org/10.1128/AAC.01789-19>.

**Copyright** © 2020 Li et al. This is an open-access article distributed under the terms of the [Creative Commons Attribution 4.0 International license](https://creativecommons.org/licenses/by/4.0/).

Address correspondence to Lei Shi, [leishi@jnu.edu.cn](mailto:leishi@jnu.edu.cn), or Pingfang Tian, [tianpf@mail.buct.edu.cn](mailto:tianpf@mail.buct.edu.cn).

**Received** 1 September 2019

**Returned for modification** 23 October 2019

**Accepted** 19 December 2019

**Accepted manuscript posted online** 23 December 2019

**Published** 21 February 2020

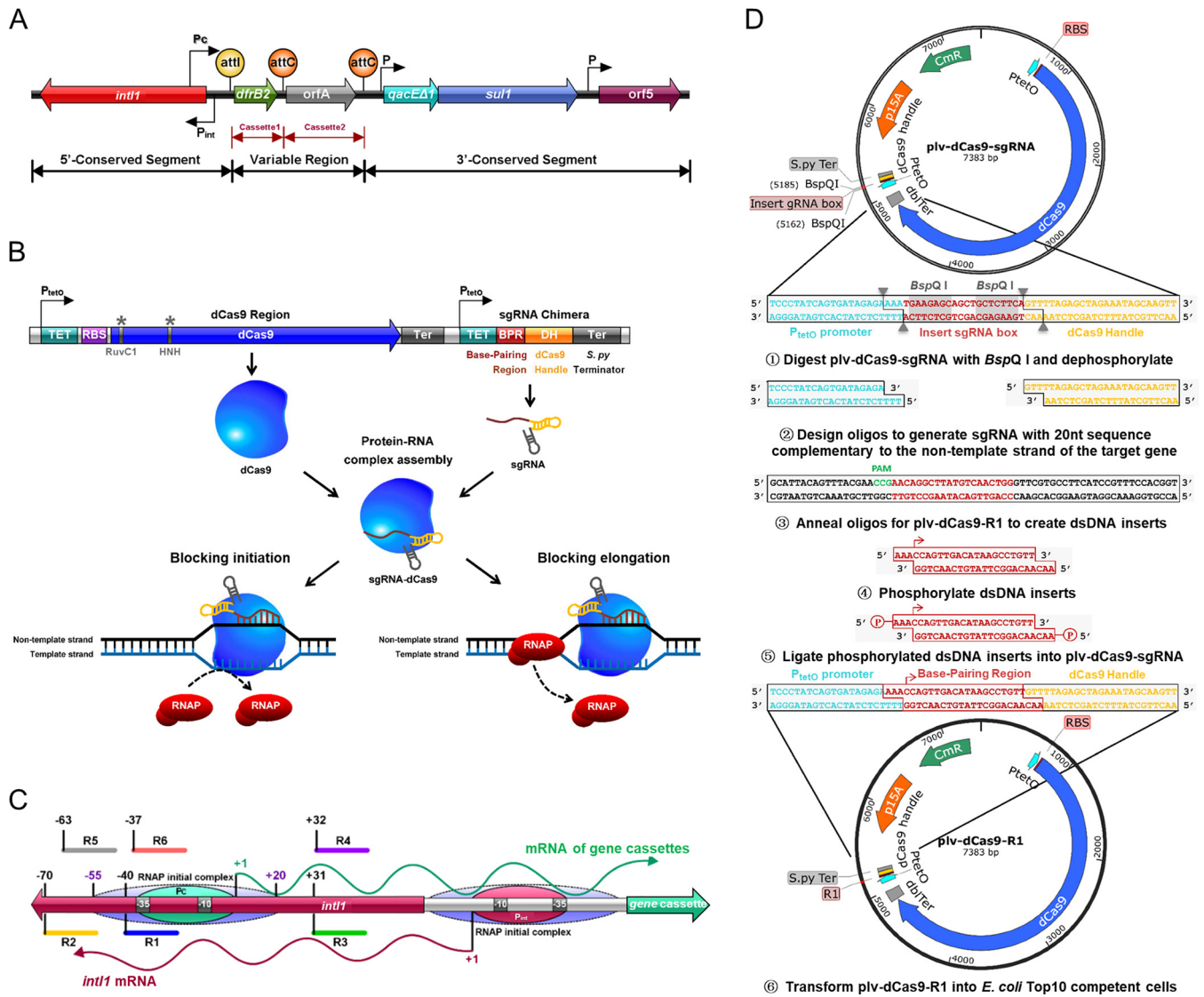


**FIG 1** Schematic diagram of engineering a CRISPRi system to repress a class 1 integron in *E. coli*. (A) Structural diagram of a class 1 integron on conjugative plasmid R388. (B) Harnessing CRISPRi to block transcription initiation and elongation. RNAP, RNA polymerase. (C) Genetic organization of *int1*, gene cassettes, Pc promoter,  $P_{int}$  promoter, and the binding sites of six sgRNAs. The six sgRNAs were designed for targeting different regions around the Pc promoter, and all target sites were located in the *Int1* integrase-coding region. The transcription start site is labeled as +1. Arabic numerals highlight the distance to the transcription start site of gene cassettes. The dotted purple oval shows the initial RNA polymerase complex. The green oval and red oval represent the Pc promoter of gene cassettes and the  $P_{int}$  promoter of *int1*, respectively. (D) Protocol for construction of CRISPRi recombinant plasmids. The same strategy is adopted to target the different regions of R388 class 1 integron in *E. coli*. The nucleotides shown with a gray background are BspQI recognition sequences, and gray triangles indicate the BspQI cutting sites. Red arrowheads indicate the transcription start sites of the base-pairing region of sgRNA.

MIs usually work with transposons, insertion sequences (ISs), and conjugative plasmids (9) and participate in the acquisition, expression, and dissemination of ARGs embedded in gene cassettes (12). Thus, integrons contribute to the transmission of bacterial antibiotic resistance (7). Structurally, almost all integrons are composed of three parts: (i) an *int1* gene (driven by a native promoter  $P_{int}$ ), which encodes an *Int1* integrase belonging to tyrosine recombinase family; (ii) a primary recombination site, *attI*, which serves as both the recognition site of *Int1* integrase and the receptor site for gene cassettes; and (iii) a Pc promoter within the *int1* coding sequence, which drives the transcription of gene cassettes inserted at the *attI* site (Fig. 1A) (13). The gene cassette usually harbors an open reading frame (ORF) surrounded by an integrase-specific recombination site, *attC* (14, 15). Typically, the integration of the gene cassette into integron is fulfilled by *Int1* integrase through site-specific recombination between *attI*

and *attC* or between two *attC* sites (16, 17). Once integrated, gene cassettes are expressed under the control of the *P<sub>c</sub>* promoter and transcribed only in a direction opposite to that of *intI* (16, 18). In addition, when subjected to stimuli (e.g., antibiotic selective pressure), the gene cassette located between two adjacent *attC* sites might be excised by *IntI* integrase, resulting in the rearrangement of internal gene cassettes or gene capture by other integrons (14, 15). The entire process involves integration, expression, and excision of gene cassettes, leading to physiological alternations or even novel genetic traits adapting to environments (3).

Among five classes of MIs (7), class 1 integrons are the most disseminated type in commensals and pathogens of humans and animals (19, 20) and have been found in other ecosystems (21, 22). Structurally, the 3' conserved segment (CS) in the class 1 integron comprises three elements: *qacEΔ1* (cationic compound disinfectant resistance gene; GenBank accession number [NG\\_048042](#)), *sul1* (sulfamethoxazole resistance gene; GenBank accession number [WP\\_000259031](#)), and *orf5* (ORF with unknown function) (Fig. 1A) (20). It is extremely challenging to eliminate class 1 integrons as their mobility allows them move onto other recipients to ensure their persistence (8, 13). To date, no efficient approach has been developed to block class 1 integrons. One exception is struvite in combination with a biochar amendment, which has been shown to suppress class 1 integrons in phyllosphere and rhizosphere soils (21). Other exceptions are treatments of residual wastewater solids, such as thermophilic anaerobic digestion, alkaline stabilization, and pasteurization. These approaches can thwart class 1 integrons in wastewater solids-amended soil (22). So far, at least 132 ARG cassettes have been identified which confer resistances to almost all types of antibiotics (14, 19). Therefore, it is highly desirable to come up with an approach suppressing class 1 integrons to counteract the devastating effects of MDRs.

CRISPR technology opens avenues for genome editing and gene regulation (23, 24). In sharp contrast to successful application in fungi, especially *Saccharomyces cerevisiae* (23, 24), CRISPR editing in bacteria is problematic due mainly to the lack of corresponding DNA repair mechanisms (25). Derived from CRISPR-Cas9, CRISPR interference (CRISPRi) consists mainly of one or several subgenomic RNAs (sgRNAs) and a catalytically dead Cas9 protein (dCas9) lacking endonuclease activity (26). With the goal of knock-down rather than knockout of a gene, CRISPRi technology does not rely on the cellular innate DNA repair machinery and thus is functional in microbes lacking a DNA repair mechanism. The CRISPRi system has been widely harnessed to retard the initiation or elongation of gene transcription (Fig. 1B) (26, 27). Notably, the CRISPRi system can simultaneously upregulate or downregulate multiple genes due to the sgRNAs which lead dCas9 to desired genomic loci (28). Considering that integron-assisted MDR involves a series of genes, CRISPRi may simultaneously interfere with multiple ARGs and thus hold great potential for prevention of bacterial infection and MDR treatment. For instance, simply by encapsulating the dCas9 and a panel of sgRNAs into nanoparticles (29, 30) and incubating these with bacteria for transformation, a wide range of ARGs could be inhibited, achieving desired therapeutic effects.

Given the above information, we conjectured that the CRISPRi system may efficiently reduce MDR by blocking class 1 integrons. Following this assumption, we developed a CRISPRi system in *Escherichia coli* C600 to curb the class 1 integron on the conjugative plasmid R388 (12). Reverse transcription and quantitative PCR (RT-qPCR) analysis were performed to assess the ability of a CRISPRi system to repress the *IntI1* integrase gene and ARGs. A microplate alamarBlue assay (MABA) and growth measurement were performed to dissect the performance of the CRISPRi system in mitigating antibiotic resistance arising from the class 1 integron. Conjugation assays were carried out to disentangle the impacts of the CRISPRi system on HGT of ARGs associated with the *IntI1* integrase-mediated integration of ARG cassettes. A titration experiment was performed to determine whether the activity of the CRISPRi system can be controlled by varying the concentration of the inducer. Finally, serial subculture experiments were conducted to investigate the reversibility and hereditary stability of a CRISPRi system.

Overall, this study aims to develop a CRISPRi system capable of repressing class 1 integron-aided MDR of *E. coli* and other bacteria.

## RESULTS

**Reduced antibiotic resistance of *E. coli* harboring a CRISPRi system.** To inactivate the class 1 integron, we constructed seven recombinant *E. coli* C600[R388/plv-dCas9-R(0–6)] strains harboring an anhydrotetracycline (aTc)-inducible CRISPRi system driven by the  $P_{tetO}$  promoter (Fig. 2A), whereby R(0–6) stands for different sgRNAs. The strain embracing sgRNA R0 was used as a control. The sgRNAs R1 to R6 were designed to inhibit the R388 class 1 integron, whereby the Pc variant was PcS with an inactive P2 promoter, and the internal ARGs were a *dfrB2* cassette for trimethoprim (TMP) resistance in the variable region and *sul1* for sulfamethoxazole (SUL) resistance in the 3' CS (Fig. 1A). Sequencing results demonstrated that all CRISPRi recombinant plv-dCas9-R(0–6) plasmids were properly constructed (see Fig. S1 in the supplemental material).

Considering that the CRISPRi system might block the initiation or elongation of gene transcription (Fig. 1B), RT-qPCR was performed to examine the transcriptional levels of the *dfrB2* cassette and *sul1*. Upon aTc induction, the sgRNA R6 targeting the –35 box of the Pc promoter on the *int1* template strand showed the highest inhibitory efficiency (97% against the *dfrB2* cassette; 84% against *sul1*). In contrast, the sgRNA R5 targeting the upstream region of the Pc promoter on the *int1* template strand exhibited the lowest inhibition efficacy (37% against the *dfrB2* cassette; 21% against *sul1*). Compared with R6, sgRNAs, including R1, R2, R3, and R4 targeting other regions in the vicinity of the Pc promoter displayed weak inhibition (60 to 80% against the *dfrB2* cassette; 30 to 73% against *sul1*). Collectively, R6 outperformed other sgRNAs in the repression of the *dfrB2* cassette and *sul1*, and the inhibition rates in descending order are  $R6 > R3 > R2 > R1 > R4 > R5$ . Furthermore, in the absence of aTc, no significant difference was observed in the mRNA levels of both the *dfrB2* cassette and *sul1* of all CRISPRi strains relative to the levels in the control strain (Fig. 2B and E).

MABA was performed to indicate whether inhibiting the *dfrB2* cassette and *sul1* could lower the phenotypical resistance of *E. coli* to TMP and SUL, respectively. In the absence of aTc, CRISPRi strains demonstrated no difference in their levels of resistance to TMP and SUL compared with those of the control strain. In contrast, upon aTc induction, the half-maximal inhibitory concentration ( $IC_{50}$ ) of TMP for all CRISPRi strains was decreased by 8-fold (64  $\mu\text{g/ml}$ ) relative to that of the control strain (512  $\mu\text{g/ml}$ ) (Fig. 2C and D). Unlike the  $IC_{50}$  of TMP, the  $IC_{50}$ s of SUL for all CRISPRi strains were reduced to various degrees. Compared with the  $IC_{50}$  of SUL for the control strain harboring sgRNA R0 (4,096  $\mu\text{g/ml}$ ), the  $IC_{50}$  of SUL for the strain employing R4 or R5 was reduced by 2-fold (2,048  $\mu\text{g/ml}$ ), while the  $IC_{50}$ s for the CRISPRi strains expressing R1 and R2 were reduced by 4-fold (1,024  $\mu\text{g/ml}$ ) and 16-fold (256  $\mu\text{g/ml}$ ), respectively. Surprisingly, the  $IC_{50}$  of SUL for a strain expressing R3 or R6 was decreased by 32-fold (128  $\mu\text{g/ml}$ ) (Fig. 2F and G). Clearly, sgRNAs R3 and R6 were more effective than other sgRNAs in mitigating antibiotic resistance, and the order of inhibition rates is  $R6 \approx R3 > R2 > R1 > R4 \approx R5$ .

Given that the CRISPRi system significantly repressed ARG transcription and antibiotic resistance, we next investigated the correlation between the transcriptional levels of ARGs (*dfrB2* cassette and *sul1*) and the  $IC_{50}$ s for the corresponding antibiotics (TMP and SUL). Results showed that the transcription of the *dfrB2* cassette was correlated with the  $IC_{50}$  of TMP (Pearson correlation coefficient of 0.8436) and that the mRNA level of *sul1* was correlated with the  $IC_{50}$  of SUL (Pearson correlation coefficient of 0.9022) (Fig. 2H and I). These results indicated that the reduced resistance to TMP and SUL was largely ascribed to CRISPRi-mediated downregulation of the *dfrB2* cassette and *sul1*, respectively. In addition, there existed a correlation between expression of the *dfrB2* cassette and *sul1* as the Pearson correlation coefficient was up to 0.9414 (Fig. 2J). Hence, we speculate that both the *dfrB2* cassette and *sul1* were controlled by the Pc promoter. Overall, the engineered CRISPRi system significantly reduced antibiotic resistance through blocking the class 1 integron in *E. coli*.



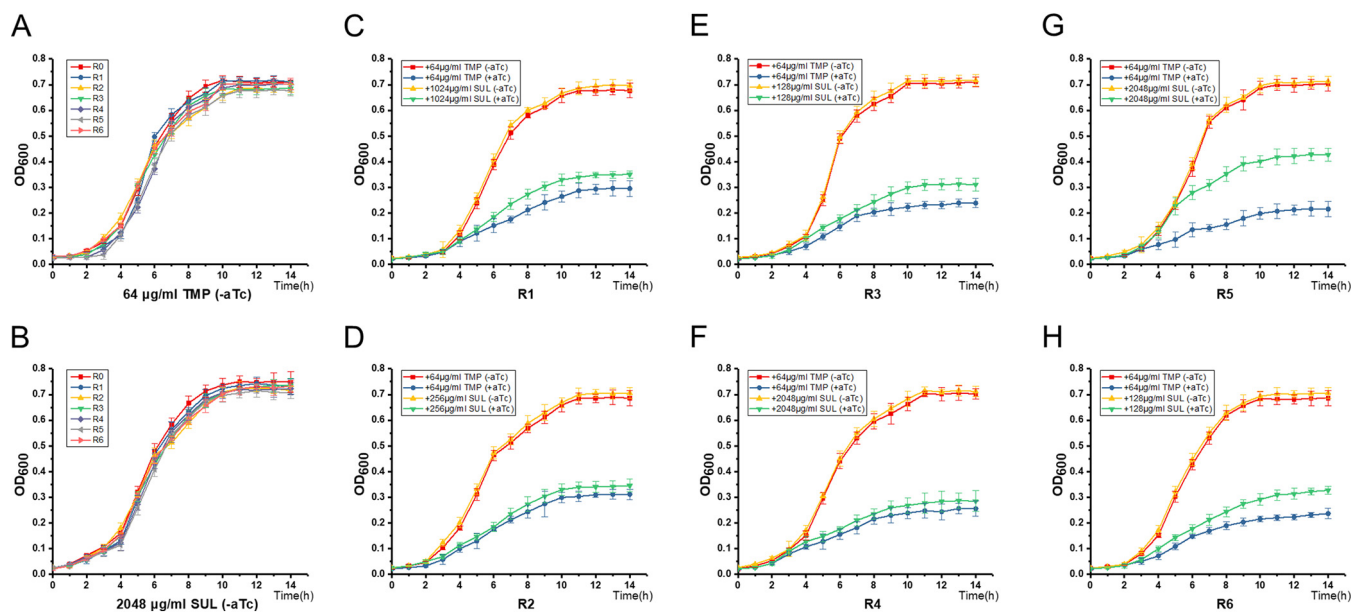


**FIG 3** Growth curves of the recombinant *E. coli* strains harboring the class 1 integron on R388 and with the CRISPRi system. (A and B) The recombinant *E. coli* strains harboring plasmid R388 and recombinant plasmid pIv-dCas9-R(0–6), which were grown in LB medium containing either TMP (A) or SUL (B) without induction of the CRISPRi system. (C to H) The recombinant *E. coli* strains harboring R388 and pIv-dCas9-R(1–6), which were cultivated in LB medium containing TMP/SUL (at the  $IC_{50}$ ) with/without aTc. TMP, trimethoprim; SUL, sulfamethoxazole;  $IC_{50}$ , half-maximal inhibitory concentration; aTc, anhydrotetracycline; R(0–6), *E. coli* C600[R388/pIv-dCas9-R(0–6)]. All data represent the means  $\pm$  standard deviations of biological triplicates.

**Suppressed growth of *E. coli* harboring a CRISPRi system.** Based on the above-described experimental results, we subsequently investigated the growth of CRISPRi strains in Luria-Bertani (LB) medium containing corresponding antibiotics. We first assessed the effects of an uninduced CRISPRi system on the growth of recombinant *E. coli* C600[R388/pIv-dCas9-R(0–6)] cultivated in LB medium containing TMP/SUL. Not surprisingly, no difference in growth rates was discovered between the CRISPRi strains and the control strain (Fig. 3A and B), indicating that the CRISPRi system has no significant impact on *E. coli* growth, and leakage expression was substantially avoided through tight control of the  $P_{tetO}$  promoter. Next, we investigated the effects of an aTc-inducible CRISPRi system on the growth of recombinant *E. coli* C600[R388/pIv-dCas9-R(1–6)] incubated in LB medium containing TMP/SUL at the concentration of the  $IC_{50}$ . Compared to uninduced strains, the aTc-induced CRISPRi strains manifested halted growth from 3 to 14 h (Fig. 3C to H). These results indicated that the CRISPRi system substantially repressed the class 1 integron-aided ARGs and in turn retarded the growth of CRISPRi strains exposed to the antibiotics tested.

**Attenuated HGT of ARGs among *E. coli* harboring a CRISPRi system.** To clarify whether the CRISPRi system impeded the class 1 integron-aided HGT of ARGs, two conjugation models were developed (Fig. 4A). The donor for each model was recombinant *E. coli* C600[R388/pIv-dCas9-R(0–6)] harboring one of the following recombinant plasmids: pINT-*aadA1* for generating an *aadA1* cassette or pINT-*aadB* for generation of an *aadB* cassette. In addition, wild-type *E. coli* J53 was employed as the recipient in each model. To begin with, we investigated the conjugation between the recipient and the control donor *E. coli* C600[R388/pIv-dCas9-R0/pINT-cassette] without induction of CRISPRi system. The “cassette” indicates different ARG cassettes. The sequencing results of *E. coli* J53(R388-*aadA1*) and *E. coli* J53(R388-*aadB*) demonstrated that the two conjugation models allowed for HGT of ARGs among *E. coli* strains (Fig. S2).

Next, we investigated the HGT rates of *aadA* and *aadB* using the two conjugation models mentioned above. In the absence of aTc, no significant difference was found between the HGT rates of all CRISPRi *E. coli* C600[R388/pIv-dCas9-R(1–6)/pINT-cassette] donor strains and the control donor. Upon aTc induction, all CRISPRi donor strains

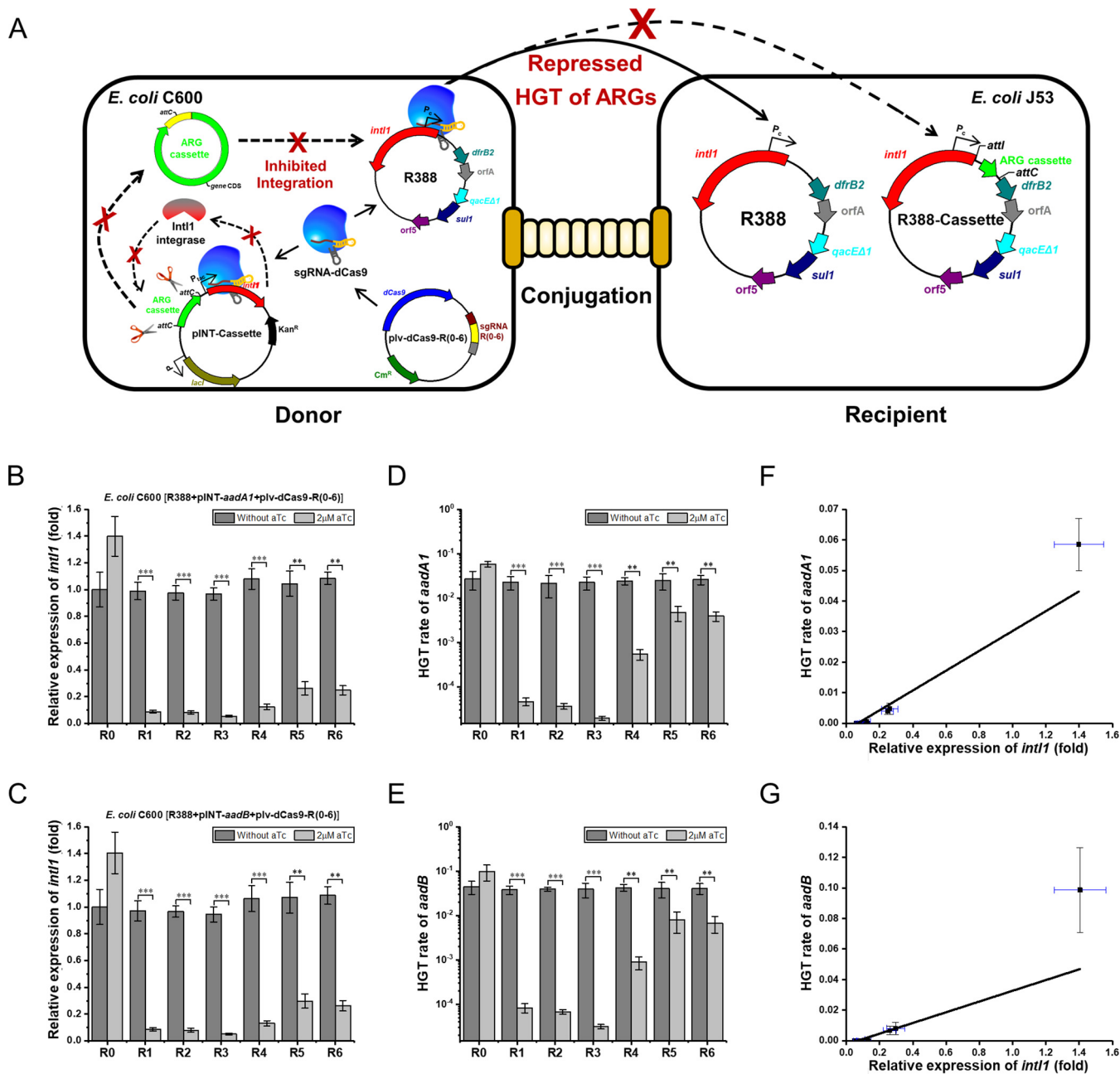


**FIG 4** Performance of the CRISPRi system in reducing the class 1 integron-associated HGT of ARGs in *E. coli*. (A) Schematic diagram of a CRISPRi system to inhibit HGT of ARGs related to the *Int11* integrase-mediated integration of ARG cassettes. (B and C) Transcription of *int11* in the recombinant *E. coli* harboring plasmid R388, recombinant plasmid plv-dCas9-R(0-6), and either pINT-*aadA1* (B) or pINT-*aadB* (C). (D and E) HGT rates of *aadA1* (D) or *aadB* (E) associated with the *Int11* integrase-mediated integration of ARG cassettes with/without aTc induction. (F and G) Correlation between *int11* transcription and the HGT rate of *aadA1* (F) or *aadB* (G). HGT, horizontal gene transfer; ARGs, antibiotic resistance genes; aTc, anhydrotetracycline; R(0-6), *E. coli* C600[R388/plv-dCas9-R(0-6)/pINT-cassette]. All data represent the means ± standard deviations of biological triplicates. \*\*,  $P < 0.01$ ; \*\*\*,  $P < 0.001$ .

showed different levels of reduction in HGT rates of ARGs. Compared with the level of the control donor, the CRISPRi donor strain expressing sgRNA R1, R2, or R3 exhibited 1,000-fold inhibition against HGT of both *aadA* and *aadB*, and the CRISPRi donor strain harboring sgRNA R4 led to an approximately 100-fold decrease in HGT. In contrast, the CRISPRi donor strain expressing R5 or R6 displayed only 10-fold decrease in HGT. Strikingly, of all sgRNAs, sgRNA R3 was most efficient in repressing HGT of ARGs, and the inhibitory rates in descending order were R3 > R2 > R1 > R4 > R6 > R5 (Fig. 4D and E).

Since HGT of ARGs in each conjugation model was related to the *Int1* integrase-involved integration of ARG cassettes, the *int1* transcription in all donors was analyzed by RT-qPCR. The *int1* transcription of the control donor harboring sgRNA R0 without aTc induction was considered to be 1. Results showed that, in each conjugation model with aTc induction, sgRNAs R1, R2, and R3 targeting the nontemplate strand of *int1* displayed 90 to 96% inhibition against *int1* transcription, while the other sgRNAs, R4, R5, and R6, targeting the template strand of *int1* exhibited only 70 to 85% inhibition against *int1* transcription. Among all sgRNAs examined, sgRNA R3 was the most effective in the downregulation of *int1* transcription, and the inhibitory rates in descending order were R3 > R2 > R1 > R4 > R6 > R5. As expected, no significant changes were observed in *int1* transcription levels when aTc was absent (Fig. 4B and C).

Given that the engineered CRISPRi system significantly attenuated both HGT of ARGs and *int1* transcription, we next explored the correlation between HGT and *int1* expression. As shown in Fig. 4F and G, the *int1* mRNA level was closely correlated with the HGT rate of *aadA1* or *aadB*. The Pearson correlation coefficients were 0.9969 and 0.9944, respectively. In other words, the inhibition efficiency of the CRISPRi system against *int1* transcription was proportional to the HGT rate of ARGs. Clearly, the CRISPRi system efficiently repressed HGT of ARGs through inhibition of the activity of the class 1 integron in *E. coli*.

**Titration of CRISPRi system.** To fully assess the engineered CRISPRi system, 2  $\mu$ M aTc was used to trigger the expression of the *dcas9* gene and sgRNA based on a previously described method (27). To determine the aTc concentration at which the CRISPRi system was adequately triggered while bacterial growth was not negatively affected, we first examined the growth of the control strain *E. coli* C600(R388/plv-dCas9-R0) cultivated in LB medium containing serial dilutions of aTc. The growth of the control strain was not remarkably halted when the aTc concentration was 0.125, 0.25, 0.5, 1, or 2  $\mu$ M. In addition, no significant difference in growth rates was observed between aTc-induced and uninduced strains in the first 5 h and after 13 h cultivation (Fig. 5A). However, when 4  $\mu$ M aTc was used to induce the CRISPRi system, the growth of the control strain was significantly retarded compared to that of the control strain without aTc induction (Fig. 5A). RT-qPCR showed that *dCas9* gene transcription relied on aTc induction and that its mRNA level peaked when the aTc concentration reached 2  $\mu$ M. Interestingly, when 2  $\mu$ M or 4  $\mu$ M aTc was used to induce the CRISPRi system, the *dcas9* mRNA level in the CRISPRi strain *E. coli* C600(R388/plv-dCas9-R3) was slightly higher than that of the control strain (Fig. 5B). Collectively, the appropriate aTc concentration for triggering the CRISPRi system is 2  $\mu$ M because at this concentration the *dcas9* gene was fully transcribed, and *E. coli* growth was not significantly halted.

Although the CRISPRi system does not cause double-stranded DNA breaks (DSBs), a low concentration of inducer is preferred as it minimizes the negative influences of the CRISPRi system on the host. To this end, we investigated the influence of serially diluted aTc on the transcriptional levels of the *dcas9* gene, the *dfrB2* cassette, *sul1*, and *int1* in recombinant *E. coli* C600(R388/plv-dCas9-R3). We focused on this CRISPRi strain because sgRNA R3 manifested the strongest inhibition on both antibiotic resistance and HGT of ARGs (Fig. 2D to G and Fig. 4D and E). A dose-response correlation was demonstrated between the *dCas9* mRNA level and aTc concentration at which the *dfrB2* cassette, *sul1*, and *int1* were transcriptionally inactivated. While a low concentration of aTc (0.125 or 0.25  $\mu$ M) did not significantly affect the level of *int1* transcription compared to that of the control, a high concentration of aTc (0.5, 1, or 2  $\mu$ M) led to a pronounced increase in the *dcas9* mRNA level, which was correlated with the remarkably repressed transcription of the *dfrB2* cassette, *sul1*, and *int1*. However, when 4  $\mu$ M aTc was used, no significant changes were observed compared with levels with 2  $\mu$ M aTc induction (Fig. 5B and C). Given these results, we investigated the correlation between the transcriptional levels of the *dfrB2* cassette, *sul1*, and *int1* and aTc at concentrations ranging from 0 to 2  $\mu$ M. Results demonstrated that the transcription

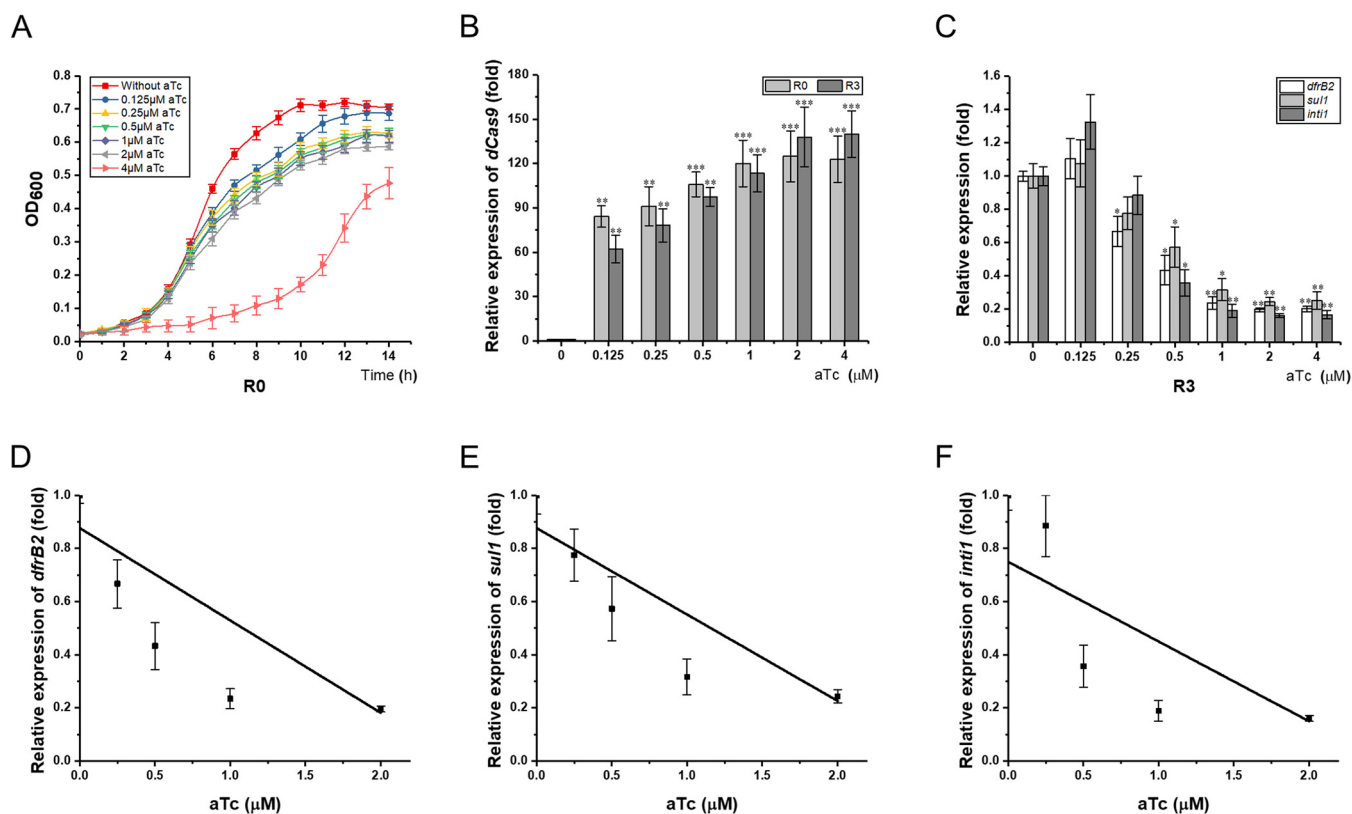


**FIG 5** Titration of CRISPRi system in *E. coli*. (A) Growth curve of the control strain upon induction with 2-fold serial concentrations of aTc ranging from 0 to 4  $\mu\text{M}$ . (B) Transcription of *dcas9* gene in recombinant *E. coli* harboring plasmid R388 and either recombinant plasmid plv-dCas9-R3 or plv-dCas9-R0 upon induction by aTc ranging from 0 to 4  $\mu\text{M}$ . (C) Transcriptional levels of the *dfrB2* cassette, *sul1*, and *int11* in the CRISPRi strain harboring sgRNA R3 upon induction by aTc at concentrations ranging from 0 to 4  $\mu\text{M}$ . (D to F) Correlation analysis between the transcription of the *dfrB2* cassette (D), *sul1* (E), or *int11* (F) and the aTc concentration ranging from 0 to 2  $\mu\text{M}$ . aTc, anhydrotetracycline; R0, *E. coli* C600(R388/plv-dCas9-R0); R3, *E. coli* C600(R388/plv-dCas9-R3). Asterisks indicate significant differences between results for aTc-treated and untreated strains (\*,  $P < 0.05$ ; \*\*,  $P < 0.01$ ; \*\*\*,  $P < 0.001$ ).

levels of the above three genes were negatively correlated with aTc concentration, with the Pearson correlation coefficients of  $-0.9243$ ,  $-0.9199$ , and  $-0.8336$ , respectively (Fig. 5D to F). Taking these results together, CRISPRi efficiency was titratable when the aTc concentration ranged from 0 to 2  $\mu\text{M}$ , and 2  $\mu\text{M}$  aTc led to the strongest CRISPRi efficacy. It is worth noting that moderate, instead of strong, aTc induction is ideal for CRISPRi activity.

#### Reversibility and hereditary stability of a CRISPRi system targeting integron.

To determine whether the CRISPRi system is reversible in *E. coli*, the strain *E. coli* C600(R388/plv-dCas9-R3) and the control strain *E. coli* C600(R388/plv-dCas9-R0) were incubated in aTc-lacking LB medium until mid-exponential phase, and the resultant strains were considered the first generation. Subsequent generations were acquired as described in Materials and Methods. The first generation of *E. coli* C600(R388/plv-dCas9-R3) was induced by aTc, resulting in the second generation. RT-qPCR analysis showed that the second-generation strain demonstrated a dramatic decrease in the transcriptional levels of the *dfrB2* cassette, *sul1*, and *int11* compared with those of the first-generation strain. Notably, when aTc was removed to acquire the third generation, the transcriptional levels of the *dfrB2* cassette, *sul1*, and *int11* were restored to those of the first-generation strain. The same manipulation was repeated for the fourth and fifth generations (Fig. 6A to C). For each generation of the control strain, whether aTc was present or absent, no significant change was observed in the mRNA levels of the *dfrB2* cassette, *sul1*, and *int11* (Fig. 6A to C). The above results indicated that the activity of the CRISPRi system was controllable and reversible in *E. coli*.

Apart from reversibility, we also investigated the hereditary stability of the CRISPRi system. To do so, we focused on the hereditary stability of recombinant *E. coli*

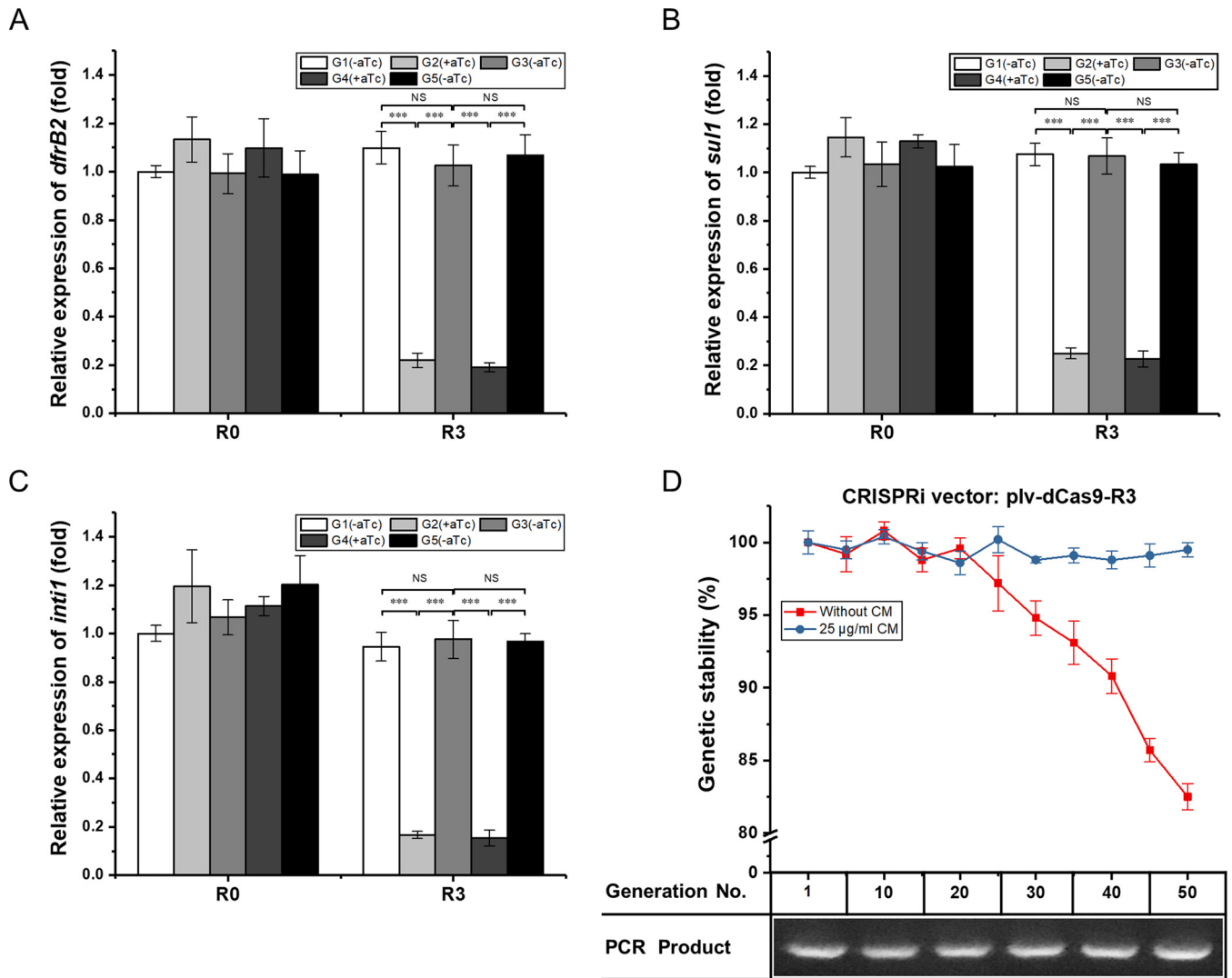


**FIG 6** Reversibility and hereditary stability of a CRISPRi system in *E. coli*. (A to C) Reversibility of transcriptional levels of the *drfB2* cassette (A), *sul1* (B), or *int11* (C) in different generations of recombinant *E. coli* harboring a CRISPRi vector exposed to aTc or not. (D) Hereditary stability and PCR analysis of recombinant plasmid plv-dCas9-R3 serially passaged in liquid culture with or without CM. The strain without exposure to CM was used as the control. aTc, anhydrotetracycline; CM, chloramphenicol; R0, *E. coli* C600(R388/plv-dCas9-R0); R3, *E. coli* C600(R388/plv-dCas9-R3). NS, not significant ( $P > 0.05$ ); \*\*\*,  $P < 0.001$ .

C600(R388/plv-dCas9-R3), which was continuously cultured in LB liquid medium containing chloramphenicol (CM), as appropriate. The same strain continuously cultured in LB liquid medium without CM was employed as the control. After 50 generations of passage in LB liquid medium containing CM, we found that all cells harbored recombinant plasmid plv-dCas9-R3. In contrast, in the absence of CM, only 82.5% of cells harbored plv-dCas9-R3 (Fig. 6D and Fig. S3). PCR analysis showed that the amplified DNA band was our desired 522-bp fragment (Fig. 6D), confirming that the colony on the LB-CM plate included plv-dCas9-R3. The above results indicated that the plv-dCas9-R3 plasmid in CM-lacking LB medium was less stable than that in CM-containing LB medium. In other words, CM is crucial for the maintenance of the engineered CRISPRi system.

**DISCUSSION**

In this work, a CRISPRi system was developed to repress the mobile class 1 integron on conjugative plasmid R388 in *E. coli* (Fig. 1). The transcriptional levels of the *drfB2* cassette and *sul1* were downregulated by 97% and 84%, respectively (Fig. 2B and E). As a result, the IC<sub>50</sub> values for TMP and SUL were reduced by 8- and 32-fold, respectively

(Fig. 2C, D, F, and G). Meanwhile, the strains showed reduced growth relative to that of the control strain harboring a CRISPRi vector but without a targeting sequence (Fig. 3C to H). Notably, the mRNA level of *int11* was downregulated by 96% (Fig. 4B and C), and the HGT rates for both *aadA1* and *aadB* were reduced by 1,000-fold (Fig. 4D and E). Among all sgRNAs examined, sgRNA R3 was most effective in reducing the activity of the class 1 integron. Furthermore, the engineered CRISPRi system is reversible (Fig. 6A to C) and genetically stable (Fig. 6D and Fig. S3), and its activity is titratable by varying the aTc concentration (Fig. 5). Based on a comprehensive consideration of the above results, we recognized that the 31 bp downstream of the Pc promoter on nontemplate strand of *int11* is the ideal target of the CRISPRi system. To our knowledge, this is the first report of harnessing a CRISPRi system to thwart the class 1 integron in *E. coli*.

In an effort to efficiently block the class 1 integron, we designed and chemically synthesized a total of six sgRNAs. We found that all six sgRNAs (R1 to R6) significantly reduced the  $IC_{50}$  of TMP, indicating that Pc promoter and its vicinity are appropriate targets of the CRISPRi system (Fig. 2C and D). Of six sgRNAs tailored to block the integron, the sgRNA R3 targeting the 31 bp downstream of the Pc promoter on the nontemplate strand of *int11* displayed the strongest inhibition on the class 1 integron. Although sgRNA R6 showed strongest inhibition on both the *dfrB2* cassette and *sul1* (Fig. 2B and E), sgRNA R3 not only displayed the strongest inhibition against HGT of ARGs but also resulted in the lowest  $IC_{50}$  values (similar to those of sgRNA R6) for both TMP and SUL (Fig. 2C, D, F, and G). Upon comprehensive consideration, we conclude that sgRNA R3 is more effective than sgRNA R6 in mitigating the integron.

Apart from the screening of powerful sgRNAs, we tried to disentangle the responses of different regions of the class 1 integron to the CRISPRi system. We found that sgRNAs R1, R2, and R3 targeting the nontemplate strand of *int11* displayed higher inhibition against HGT of ARGs than sgRNAs R4, R5, and R6 targeting the template strand of *int11* (Fig. 4D and E). This result is consistent with previous study (26). For the CRISPRi strain recruiting sgRNA R3, the correlation coefficient between aTc concentration and *int11* transcription was less than that between aTc concentration and the *dfrB2* cassette transcription (Fig. 5D to F). This indicated that the promoter of the *dfrB2* cassette is more easily inhibited than the coding sequence of *int11*. With regard to ARGs in the class 1 integron, the *dfrB2* cassette was transcriptionally synchronized with *sul1* (Fig. 2J), suggesting that the Pc promoter drove the transcription of both the *dfrB2* cassette and the *sul1* gene located in the 3' CS of the integron. This finding is consistent with the notion that *sul1* is originally an inserted ARG (12), and it may permanently reside in the integron if it benefits the survival of the host cell (31). Unlike the  $IC_{50}$  of TMP, that of SUL for all CRISPRi strains was reduced in various degrees (Fig. 2C and F). A previous study (6) suggests that the two *attC* sites between the Pc promoter and *sul1* (Fig. 1A) might form a stable stem-loop which impedes ribosome progression along polycistronic RNA and thus reduces *sul1* translation.

This work provides insights for future management of MDR pathogens. For instance, based on experimentally validated sgRNA R3, a vehicle encompassing sgRNA R3 and the dCas9 could be prepared and delivered to desired settings and subsequently respond to cues such as pH (30), light (29, 32), or magnetism (33) for eliciting a CRISPRi system. In fact, CRISPR delivery systems have been under construction recently (29, 30, 32, 33). For instance, one group from Nanjing University attempted to cure a tumor by a near-infrared (NIR) light-responsive nano carrier of CRISPR-Cas9 (32). Shortly afterwards, another group from Rice University reported spatial control of CRISPR editing through an artificial magnetic-field-driven baculoviral vector (33). These interdisciplinary studies are broadening the applications of the CRISPR system (34). In addition to the aforementioned nanoparticles (32, 33), the CRISPR system can be delivered by conjugative plasmids (35, 36), phagemids (35), mobile genomic islands (37), or transposons (38, 39). Given this information, we envision that the CRISPR system may be fused to an integron, resulting in a chimeric integron which is mobile. To do so, the original 3' CS genes of integrons can be replaced by Cas9/dCas9 genes and sgRNAs that specially target virulence and biofilm-associated genes. More broadly, this artificial integron

could be harnessed for microbial breeding (40), targeted killing of pathogens (41), epidemiological forecasting when combined with fluorescent label (42), and monitoring of anthropogenic pollution (43). Overall, this study provides valuable insights for both mitigation and utilization of a class 1 integron.

## MATERIALS AND METHODS

**Strains, vectors, and medium.** The strains and vectors used in this study are listed in Table S1 in the supplemental material. Wild-type *E. coli* C600 was used as the host strain for harboring vectors, and *E. coli* J53 was employed as the recipient strain to examine bacterial conjugation. Conjugative plasmid R388 (GenBank accession number [NC\\_028464](#)) harbors a class 1 integron. Vector plv-dCas9-sgRNA (27) was used as the backbone of CRISPRi system. The engineered plasmid pINT-cassette was used for gene cassette insertion and *Int1* integrase expression. All *E. coli* strains were grown in Luria-Bertani (LB) medium containing 10 g/liter tryptone, 5 g/liter yeast extract, 10 g/liter sodium chloride, and antibiotics and inducers as appropriate. Shake-flask cultivation was carried out in a rotatory shaker at 180 rpm. Positive clones were screened by LB plates (LB medium with 1.5% agar) containing antibiotics and inducers, as appropriate, at 37°C.

**Development of a CRISPRi system to inhibit a class 1 integron in *E. coli*.** Wild-type *E. coli* C600 was transformed with conjugative plasmid R388, resulting in recombinant *E. coli* C600(R388). To inhibit R388 class 1 integron, *E. coli* C600(R388) was transformed with the CRISPRi vector plv-dCas9-R(0–6), resulting in recombinant *E. coli* C600[R388/plv-dCas9-R(0–6)], where the plv-dCas9-R(0–6) plasmids were derived from plv-dCas9-sgRNA (27) and where R(0–6) stands for different sgRNAs. The plasmid plv-dCas9-sgRNA (27) contains an inactive dCas9 gene from *Streptococcus pyogenes* and an sgRNA chimera, both of which are driven by an aTc-inducible  $P_{tetO}$  promoter. The sgRNA chimera consists of three parts: (i) a 20-bp DNA fragment complementary to the target locus, named the base-pairing region (BPR); (ii) a 42-bp hairpin region, named dCas9 handle (DH), for dCas9 binding; and (iii) a 40-bp terminator designated *rrnB* (Ter) (Fig. 1B) (26). The BspQI sites in plasmid plv-dCas9-sgRNA were used for directional cloning of any sgRNA into this vector without leaving a scar. After plv-dCas9-sgRNA was digested by BspQI, two different 3-nucleotide (nt) overhangs were formed, and the BspQI sites were removed from the vector. Taking the construction of recombinant plasmid plv-dCas9-R1 as an example, two complementary oligonucleotides, 20 bases of sequence homologous to the target loci and 3 bases at the 5' end of each oligonucleotide matching the BspQI-digested vector, were annealed, phosphorylated, and cloned into plv-dCas9-sgRNA (Fig. 1D). This protocol allows for plug-and-play of sgRNAs.

The target locus should be immediately downstream of the sequence CCX, the reverse complement of an NGG protospacer adjacent motif (PAM) sequence (44). According to this, we selected the CCX around the Pc promoter to determine the target sequence in R388 class 1 integron. A total of seven sgRNAs were designed. Both sgRNA R1 and R6 were designed to target the –35 box of the Pc promoter, the sgRNAs R2 and R5 target the upstream region of the Pc promoter, and sgRNA R3 and sgRNA R4 target the downstream region of the Pc promoter as well as the region between the transcription start site and the initiation codon of the *dfxB2* cassette. Notably, all of the above sgRNAs were designed to target the coding region of the *Int1* integrase. While the sgRNAs R1, R2, and R3 were designed to target the nontemplate strand of *int1*, sgRNAs R4, R5, and R6 were designed to target the template strand of *int1* (Fig. 1C). The sgRNA R0 without targeting any sequence in all experimental strains was prepared as the control. In addition, a BLAST search was performed to examine the specificity of sgRNAs. Subsequently, all oligonucleotides listed in Table S2 for generating sgRNAs were synthesized to form recombinant plv-dCas9-R(0–6) plasmids, which were individually transformed into competent *E. coli* cells and confirmed by colony PCR and sequencing.

**Construction of recombinant plasmids for gene cassette insertion and *Int1* integrase expression.** The recombinant plasmid pINT-cassette harbors a promoter-lacking ARG cassette and an *int1* gene (encoding class 1 integron integrase *Int1*; GenBank accession number [WP\\_000845048](#)) with an isopropyl- $\beta$ -D-thiogalactopyranoside (IPTG)-inducible *tac* promoter. Notably, the ARG embedded in the gene cassette follows the same coding orientation as *int1*. The *tac* promoter along with multiple cloning sites were synthesized and inserted into vector pET-28a between BglIII and NcoI sites to generate vector pEtac-28a. In this process, one BmgBI site was introduced into pEtac-28a to facilitate subsequent insertion of an ARG cassette (Fig. S4A). The *int1* was amplified by PCR from plasmid R388 with primers Ndel-*int1*-F/*int1*-XhoI-R and then cloned into Ndel-XhoI doubly digested vector pEtac-28a, resulting in vector ptaINT (Fig. S4B). Next, the *aadA1* cassette was amplified from the *Salmonella* sp. strain s010 class 1 integron (GenBank accession number [AB285480](#)) with primers BglIII-*aadA1*-F/*aadA1*-BmgBI-R and then inserted into BglIII-BmgBI doubly digested vector ptaINT, resulting in recombinant plasmid pINT-*aadA1* (Fig. S4C). The *aadB* cassette from the *Salmonella* sp. strain s084 class 1 integron (GenBank accession number [AB285479](#)) was amplified by PCR with BglIII-*aadB*-F/*aadB*-BmgBI-R and then cloned into BglIII-BmgBI doubly digested vector ptaINT, yielding recombinant plasmid pINT-*aadB* (Fig. S4D). This framework allowed for the generation of an episomal ARG cassette mediated by *Int1* integrase following IPTG induction. All recombinant plasmids were transformed into competent cells and confirmed by colony PCR and sequencing. All primers for pINT-cassette construction are listed in Table S2.

**Determination of antibiotic susceptibility.** The recombinant *E. coli* C600[R388/plv-dCas9-R(0–6)] strains were examined for their antibiotic susceptibility by MABA (45). The strain *E. coli* ATCC 25922 was employed as the quality control. Twofold serial dilutions of specific antibiotics were carried out in a 96-well plate containing 100  $\mu$ l of Muller-Hinton (MH) medium per well. The aforementioned strains were first precultured at 37°C with 180 rpm shaking until an optical density at 600 nm ( $OD_{600}$ ) of 0.6 prior to

inoculation in MH medium. The turbidity was adjusted to McFarland standard no. 0.5 and further diluted 100-fold. Next, 100  $\mu$ l of broth was added to each well. In addition, the growth control of each strain and an aseptic control were employed. To trigger the CRISPRi system, aTc was added to a final concentration of 2  $\mu$ M. Each strain grown in medium devoid of aTc was used as a reference. Plates were cultured at 37°C for 12 h, at which point 20  $\mu$ l of alamarBlue (Invitrogen) was added to each well. Plates were incubated at 37°C for an additional 6 h and then analyzed with a fluorescence plate reader (excitation at 540 nm/emission at 595 nm; Elx800 plate reader). The lowest concentration of an antibiotic that reduced the fluorescence level to 50% of that of the growth control devoid of antibiotics was considered the IC<sub>50</sub>. The IC<sub>50</sub> experiments were performed in triplicate.

**RNA Isolation and RT-qPCR.** Tested strains were grown in LB medium for 8 h and then harvested for subsequent RNA extraction using RNAiso Plus (TaKaRa). Absorbance values at 260 and 280 nm were measured by a Nanodrop instrument to determine the quantity and purity of RNA. Quantitative PCR (qPCR) of RNA without reverse transcription (RT) was performed to exclude the effects of genomic DNA contamination. RT-qPCR was carried out using a PrimeScript RT reagent kit (TaKaRa) and SYBR Premix Ex Taq II (TaKaRa). The qPCR was conducted using an Applied Biosystems 7300 real-time PCR system with Relative Expression Software Tool 2009, version 2.0.13. The RT reaction was performed with 100 ng of RNA isolated as described above in a 20- $\mu$ l final reaction volume. The primers for RT-qPCR analysis were designed by Primer Premier, version 5.0, software to generate amplicons of 90 to 110 nt (Table S2). The slope of the standard curve of serially diluted cDNA showed that the amplification efficiencies of all primer pairs were higher than 99%. The qPCR data were analyzed using the  $\Delta\Delta C_T$  method (where  $C_T$  is threshold cycle) with *E. coli* 16S rRNA as an internal control. All samples were prepared in triplicate to investigate each target sequence.

**Determination of bacterial growth.** The recombinant *E. coli* C600[R388/plv-dCas9-R(0–6)] was first precultured overnight in LB medium containing 25  $\mu$ g/ml CM and 64  $\mu$ g/ml TMP (at 37°C with shaking at 180 rpm) and then diluted to an OD<sub>600</sub> of 0.01. To elucidate the effects of a CRISPRi system on cell growth, 200  $\mu$ l of broth was added into a 96-well plate containing 64  $\mu$ g/ml TMP and 2,048  $\mu$ g/ml SUL, respectively, but without aTc. To disentangle the effects of the CRISPRi system on the growth of recombinant *E. coli* C600[R388/plv-dCas9-R(1–6)], 200  $\mu$ l of broth was inoculated into a 96-well plate containing 2  $\mu$ M aTc and TMP or SUL at the IC<sub>50</sub> level. Each strain grown in medium devoid of aTc was used as a control. To investigate the growth of the control strain *E. coli* C600(R388/plv-dCas9-R0) subjected to different degrees of CRISPRi induction, 200  $\mu$ l of broth was cultivated in a 96-well plate containing 64  $\mu$ g/ml TMP and 2-fold serial dilutions of aTc from 0.125 to 4  $\mu$ M. All 96-well plates were placed in a shaker at 37°C and cultivated for 14 h. Cell concentration was measured every 1 h using a microplate reader (Elx800).

**Bacterial conjugation.** *E. coli* C600[R388/plv-dCas9-R(0–6)] was transformed with the aforementioned recombinant plasmid pINT-cassette, yielding donor *E. coli* C600[R388/pINT-cassette/plv-dCas9-R(0–6)]. Since plasmids R388, plv-dCas9-R(0–6), and pINT-cassette possess distinct replication origins, they are compatible with each other in *E. coli*. To examine the HGT of ARGs from the above donor strain to the recipient *E. coli* J53, conjugation experiments (17) were performed by the method of filter mating as described previously (35). The donors were incubated overnight in LB broth at 37°C and then diluted 100-fold with fresh medium containing 25  $\mu$ g/ml CM, 25  $\mu$ g/ml kanamycin (KAN), and 32  $\mu$ g/ml TMP. After 4 h of cultivation, 2  $\mu$ M aTc and 0.5 mM IPTG were simultaneously added into the donor to facilitate the integration of ARG cassettes into the R388 class 1 integron upon CRISPRi induction. Each donor received only 0.5 mM IPTG for use as a reference. The recipient was cultivated overnight in LB medium and then diluted 100-fold with fresh medium containing 100  $\mu$ g/ml sodium azide (NaN<sub>3</sub>). When the OD<sub>600</sub> reached 1.0, the donor and recipient strains were pelleted and resuspended with sterile phosphate-buffered saline (PBS). Subsequently, the donor and recipient strains were mixed at a ratio of 3:1. After the mixture was pelleted and resuspended in 20  $\mu$ l of PBS, filter mating was carried out by spotting the mixture onto a 0.45- $\mu$ m-pore-size filter (Millipore) on an LB plate. After 16 to 18 h of conjugation, cells were harvested by vigorously vortexing the filter in 1 ml of aseptic PBS. The mixture was serially diluted using PBS and plated onto LB agar containing 1,024  $\mu$ g/ml SUL and 100  $\mu$ g/ml NaN<sub>3</sub> for screening total transconjugants with R388 plus those with R388-*aadA1* or R388-*aadB*. As the genes *aadA1* and *aadB* confer resistance to streptomycin (STR) and gentamicin (GEN), respectively, the mixture was transferred to an LB plate containing 1,024  $\mu$ g/ml SUL, 25  $\mu$ g/ml STR, and 100  $\mu$ g/ml NaN<sub>3</sub> to screen for transconjugant *E. coli* J53(R388-*aadA1*). In parallel, the mixture was plated onto an LB plate containing 1,024  $\mu$ g/ml SUL, 25  $\mu$ g/ml GEN, and 100  $\mu$ g/ml NaN<sub>3</sub> to screen for transconjugant *E. coli* J53(R388-*aadB*). The HGT rate of *aadA1* or *aadB* was defined as the ratio of transconjugants with R388-*aadA1* or R388-*aadB* to total transconjugants. The donor and recipient strains were independently screened on triple-resistance plates to exclude the effects of spontaneous mutation on the mating assay. To unravel whether ARGs could move from the donor to the recipient, a conjugation experiment was first performed between the recipient *E. coli* J53 and the control donor *E. coli* C600(R388/plv-dCas9-R0/pINT-cassette) without CRISPRi induction. The genetic identity of transconjugants with R388-*aadA1* or R388-*aadB* was investigated by PCR using the specific primers Integration-CX-F/*aadA1*-CX-R to amplify *intI1-attI-aadA1* in transconjugant *E. coli* J53(R388-*aadA1*) and Integration-CX-F/*aadB*-CX-R to amplify *intI1-attI-aadB* in transconjugant *E. coli* J53(R388-*aadB*). All primers used for sequencing are listed in Table S2.

**Serial passage experiments.** To determine whether this CRISPRi system is reversible, the first generation of recombinant *E. coli* C600(R388) harboring either recombinant plasmid plv-dCas9-R0 or plv-dCas9-R3 was cultivated in LB medium without aTc until the OD<sub>600</sub> reached 1.0. Next, 1% broth was transferred to LB medium containing 2  $\mu$ M aTc, yielding the second generation of *E. coli* strains, and incubated until an OD<sub>600</sub> of 1 was reached, and the cells were washed with fresh PBS buffer. Next, 1%

of a second-generation strain was grown in LB medium devoid of aTc to acquire the third generation. After the culture reached an OD<sub>600</sub> of 1.0, the third-generation strain was pelleted, resuspended in aseptic PBS, and diluted 100-fold with aTc-containing LB medium to acquire the fourth generation, which was incubated as described for the previous rounds to form the fifth generation. After 8 h of cultivation, the transcriptional levels of the *dfrB2* cassette, *sul1*, and *int1* in different generations of strains were tested.

To investigate the hereditary stability of the CRISPRi system, the recombinant plasmid plv-dCas9-R3 was tested as reported previously (46), with minor modifications. Plasmid stability was assessed by subculture in liquid medium. The strain *E. coli* C600(R388/plv-dCas9-R3) was precultured overnight in LB medium containing 25 µg/ml CM (37°C and shaking at 180 rpm) and subsequently diluted 100-fold with fresh medium containing 25 µg/ml CM. From that, 1 ml was diluted in CM-lacking LB medium and was used as the reference. Serial passaging was performed every 12 h as follows. The CM-treated strain was sampled and diluted 100-fold by fresh medium containing CM. In contrast, the reference was sampled and diluted by LB medium without CM. Subsequently, aliquots of samples were obtained from the 1st, 10th, 20th, 30th, 40th, and 50th generations and serially diluted, spread, and enumerated in LB plates containing 25 µg/ml CM. The LB plates without CM were used as controls. The hereditary stability of vector plv-dCas9-R3 was plotted as a fraction of plasmid-containing cells for each 10 generations, which was evaluated by the colony number on LB-CM plates divided by that on LB plates without CM. The single colony surviving on LB-CM plates of different generations was confirmed by PCR using primers BspQI-R3-F/sgRNA-CX-R. Absence of a PCR product was considered plasmid loss. The experiments investigating reversibility and hereditary stability were performed in triplicate.

**Statistical analysis.** An *F* test of two samples for variance was performed. Significance of the differences (*P* values) was calculated using unpaired two-tailed *t* tests for equal or unequal variance. All tests were performed by the data analysis software GraphPad Prism, version 5.0.

## SUPPLEMENTAL MATERIAL

Supplemental material is available online only.

**SUPPLEMENTAL FILE 1**, PDF file, 1.2 MB.

## ACKNOWLEDGMENTS

This work was supported by grants from the National Natural Science Foundation of China (no. 31571934), National Key Research and Development Program of China (no. 2018YFA0901800), High Technology Research and Development Program (863 Program) (no. 2015AA021003), and National Natural Science Foundation of China (no. 21476011).

We thank George Guoqiang Chen from Tsinghua University for providing vector plv-dCas9-sgRNA. We thank Geran Tian from the University of International Business and Economics for polishing the manuscript.

## REFERENCES

- Levy SB, Marshall B. 2004. Antibacterial resistance worldwide: causes, challenges and responses. *Nat Med* 10(Suppl 12):S122–S129. <https://doi.org/10.1038/nm1145>.
- Centers for Disease Control and Prevention. 2013. Antibiotic resistance threats in the United States, 2013. CDC, Atlanta, Georgia.
- Top EM, Springael D. 2003. The role of mobile genetic elements in bacterial adaptation to xenobiotic organic compounds. *Curr Opin Biotechnol* 14:262–269. [https://doi.org/10.1016/S0958-1669\(03\)00066-1](https://doi.org/10.1016/S0958-1669(03)00066-1).
- Baharoglu Z, Bikard D, Mazel D. 2010. Conjugative DNA transfer induces the bacterial SOS response and promotes antibiotic resistance development through integron activation. *PLoS Genet* 6:e1001165. <https://doi.org/10.1371/journal.pgen.1001165>.
- Mitsuhashi S, Harada K, Hashimoto H, Egawa R. 1961. On the drug-resistance of enteric bacteria. 4. Drug-resistance of *Shigella* prevalent in Japan. *Jpn J Exp Med* 31:47–52.
- Escudero JA, Loot C, Nivina A, Mazel D. 2015. The integron: adaptation on demand. *Microbiol Spectr* 3:MDNA3-0019-2014. <https://doi.org/10.1128/microbiolspec.MDNA3-0019-2014>.
- Gillings MR. 2014. Integrons: past, present, and future. *Microbiol Mol Biol Rev* 78:257–277. <https://doi.org/10.1128/MMBR.00056-13>.
- Engelstadter J, Harms K, Johnsen PJ. 2016. The evolutionary dynamics of integrons in changing environments. *ISME J* 10:1296–1307. <https://doi.org/10.1038/ismej.2015.222>.
- Mazel D. 2006. Integrons: agents of bacterial evolution. *Nat Rev Microbiol* 4:608–620. <https://doi.org/10.1038/nrmicro1462>.
- Partridge SR. 2011. Analysis of antibiotic resistance regions in Gram-negative bacteria. *FEMS Microbiol Rev* 35:820–855. <https://doi.org/10.1111/j.1574-6976.2011.00277.x>.
- Boucher Y, Labbate M, Koenig JE, Stokes HW. 2007. Integrons: mobilizable platforms that promote genetic diversity in bacteria. *Trends Microbiol* 15:301–309. <https://doi.org/10.1016/j.tim.2007.05.004>.
- Stokes HW, Hall RM. 1989. A novel family of potentially mobile DNA elements encoding site-specific gene-integration functions: integrons. *Mol Microbiol* 3:1669–1683. <https://doi.org/10.1111/j.1365-2958.1989.tb00153.x>.
- Cambray G, Guerout AM, Mazel D. 2010. Integrons. *Annu Rev Genet* 44:141–166. <https://doi.org/10.1146/annurev-genet-102209-163504>.
- Partridge SR, Tsafnat G, Coiera E, Iredell JR. 2009. Gene cassettes and cassette arrays in mobile resistance integrons. *FEMS Microbiol Rev* 33:757–784. <https://doi.org/10.1111/j.1574-6976.2009.00175.x>.
- Bouvier M, Ducos-Galand M, Loot C, Bikard D, Mazel D. 2009. Structural features of single-stranded integron cassette *attC* sites and their role in strand selection. *PLoS Genet* 5:e1000632. <https://doi.org/10.1371/journal.pgen.1000632>.
- Hall RM, Collis CM. 1995. Mobile gene cassettes and integrons: capture and spread of genes by site-specific recombination. *Mol Microbiol* 15:593–600. <https://doi.org/10.1111/j.1365-2958.1995.tb02368.x>.
- Partridge SR, Recchia GD, Scaramuzzi C, Collis CM, Stokes HW, Hall RM. 2000. Definition of the *attI* site of class 1 integrons. *Microbiology* 146:2855–2864. <https://doi.org/10.1099/00221287-146-11-2855>.
- Hall RM, Collis CM. 1995. Expression of antibiotic resistance genes in the integrated cassettes of integrons. *Antimicrob Agents Chemother* 39:155–162. <https://doi.org/10.1128/AAC.39.1.155>.

19. Ghaly TM, Chow L, Asher AJ, Waldron LS, Gillings MR. 2017. Evolution of class 1 integrons: mobilization and dispersal via food-borne bacteria. *PLoS One* 12:e0179169. <https://doi.org/10.1371/journal.pone.0179169>.
20. Lacotte Y, Ploy MC, Raheison S. 2017. Class 1 integrons are low-cost structures in *Escherichia coli*. *ISME J* 11:1535–1544. <https://doi.org/10.1038/ismej.2017.38>.
21. An XL, Chen QL, Zhu D, Su JQ. 2018. Distinct effects of struvite and biochar amendment on the class 1 integron antibiotic resistance gene cassettes in phyllosphere and rhizosphere. *Sci Total Environ* 631–632: 668–676. <https://doi.org/10.1016/j.scitotenv.2018.03.034>.
22. Burch TR, Sadowsky MJ, LaPara TM. 2017. Effect of different treatment technologies on the fate of antibiotic resistance genes and class 1 integrons when residual municipal wastewater solids are applied to soil. *Environ Sci Technol* 51:14225–14232. <https://doi.org/10.1021/acs.est.7b04760>.
23. Wright AV, Nunez JK, Doudna JA. 2016. Biology and applications of CRISPR systems: harnessing nature's toolbox for genome engineering. *Cell* 164:29–44. <https://doi.org/10.1016/j.cell.2015.12.035>.
24. Cernak P, Estrela R, Poddar S, Skerker JM, Cheng Y-F, Carlson AK, Chen B, Glynn VM, Furlan M, Ryan OW, Donnelly MK, Arkin AP, Taylor JW, Cate JHD, Cernak P, Estrela R, Poddar S, Skerker JM, Cheng Y-F, Carlson AK, Chen B, Glynn VM, Furlan M, Ryan OW, Donnelly MK, Arkin AP, Taylor JW, Cate JHD. 2018. Engineering *Kluyveromyces marxianus* as a robust synthetic biology platform host. *mBio* 9:e01410-18. <https://doi.org/10.1128/mBio.01410-18>.
25. Cong L, Ran FA, Cox D, Lin SL, Barretto R, Habib N, Hsu PD, Wu XB, Jiang WY, Marraffini LA, Zhang F. 2013. Multiplex genome engineering using CRISPR/Cas systems. *Science* 339:819–823. <https://doi.org/10.1126/science.1231143>.
26. Qi LS, Larson MH, Gilbert LA, Doudna JA, Weissman JS, Arkin AP, Lim WA. 2013. Repurposing CRISPR as an RNA-guided platform for sequence-specific control of gene expression. *Cell* 152:1173–1183. <https://doi.org/10.1016/j.cell.2013.02.022>.
27. Lv L, Ren YL, Chen JC, Wu Q, Chen GQ. 2015. Application of CRISPRi for prokaryotic metabolic engineering involving multiple genes, a case study: controllable P(3HB-co-4HB) biosynthesis. *Metab Eng* 29:160–168. <https://doi.org/10.1016/j.ymben.2015.03.013>.
28. Mougias I, Bosma EF, de Vos WM, van Kranenburg R, van der Oost J. 2016. Next generation prokaryotic engineering: the CRISPR-Cas toolkit. *Trends Biotechnol* 34:575–587. <https://doi.org/10.1016/j.tibtech.2016.02.004>.
29. Shao J, Wang M, Yu G, Zhu S, Yu Y, Heng BC, Wu J, Ye H. 2018. Synthetic far-red light-mediated CRISPR-dCas9 device for inducing functional neuronal differentiation. *Proc Natl Acad Sci U S A* 115:E6722–E6730. <https://doi.org/10.1073/pnas.1802448115>.
30. Liu Q, Zhao K, Wang C, Zhang Z, Zheng C, Zhao Y, Zheng Y, Liu C, An Y, Shi L, Kang C, Liu Y. 2019. Multistage delivery nanoparticle facilitates efficient CRISPR/dCas9 activation and tumor growth suppression *in vivo*. *Adv Sci (Weinh)* 6:1801423. <https://doi.org/10.1002/adv.201801423>.
31. Bennett PM. 1999. Integrons and gene cassettes: a genetic construction kit for bacteria. *J Antimicrob Chemother* 43:1–4. <https://doi.org/10.1093/jac/43.1.1>.
32. Yong CP, Jing JY, Xiao WL, Xin LL, Xue QL, Jian Y. 2019. Near-infrared upconversion-activated CRISPR-Cas9 system: a remote-controlled gene editing platform. *Sci Adv* 5:eaav7199.
33. Zhu H, Zhang L, Tong S, Lee CM, Deshmukh H, Bao G. 2019. Spatial control of *in vivo* CRISPR-Cas9 genome editing via nanomagnets. *Nat Biomed Eng* 3:126–136. <https://doi.org/10.1038/s41551-018-0318-7>.
34. Lyu Y, He S, Li J, Jiang Y, Sun H, Miao Y, Pu K. 2019. A photolabile semiconducting polymer nanotransducer for near-infrared regulation of CRISPR/Cas9 gene editing. *Angew Chem Int Ed Engl* 58:18197–18201. <https://doi.org/10.1002/anie.201909264>.
35. Citorik RJ, Mimee M, Lu TK. 2014. Sequence-specific antimicrobials using efficiently delivered RNA-guided nucleases. *Nat Biotechnol* 32: 1141–1145. <https://doi.org/10.1038/nbt.3011>.
36. Sharma AK, Nymark M, Sparstad T, Bones AM, Winge P. 2018. Transgene-free genome editing in marine algae by bacterial conjugation - comparison with biolistic CRISPR/Cas9 transformation. *Sci Rep* 8:14401. <https://doi.org/10.1038/s41598-018-32342-0>.
37. Ram G, Ross HF, Novick RP, Rodriguez-Pagan I, Jiang D. 2018. Conversion of staphylococcal pathogenicity islands to CRISPR-carrying antibacterial agents that cure infections in mice. *Nat Biotechnol* 36:971–976. <https://doi.org/10.1038/nbt.4203>.
38. Strecker J, Ladha A, Gardner Z, Schmid-Burgk JL, Makarova KS, Koonin EV, Zhang F. 2019. RNA-guided DNA insertion with CRISPR-associated transposases. *Science* 365:48–53. <https://doi.org/10.1126/science.aax9181>.
39. Klompe SE, Vo PLH, Halpin-Healy TS, Sternberg SH. 2019. Transposon-encoded CRISPR-Cas systems direct RNA-guided DNA integration. *Nature* 571:219–225. <https://doi.org/10.1038/s41586-019-1323-z>.
40. Huang H, Chai C, Yang S, Jiang W, Gu Y. 2019. Phage serine integrase-mediated genome engineering for efficient expression of chemical biosynthetic pathway in gas-fermenting *Clostridium ljungdahlii*. *Metab Eng* 52:293–302. <https://doi.org/10.1016/j.ymben.2019.01.005>.
41. Bikard D, Euler CW, Jiang W, Nussenzweig PM, Goldberg GW, Duportet X, Fischetti VA, Marraffini LA. 2014. Exploiting CRISPR-Cas nucleases to produce sequence-specific antimicrobials. *Nat Biotechnol* 32: 1146–1150. <https://doi.org/10.1038/nbt.3043>.
42. Deng W, Shi X, Tjian R, Lionnet T, Singer RH. 2015. CASFISH: CRISPR/Cas9-mediated *in situ* labeling of genomic loci in fixed cells. *Proc Natl Acad Sci U S A* 112:11870–11875. <https://doi.org/10.1073/pnas.1515692112>.
43. Gillings MR, Gaze WH, Pruden A, Smalla K, Tiedje JM, Zhu YG. 2015. Using the class 1 integron-integrase gene as a proxy for anthropogenic pollution. *ISME J* 9:1269–1279. <https://doi.org/10.1038/ismej.2014.226>.
44. Singh AK, Carette X, Potluri LP, Sharp JD, Xu R, Priscic S, Husson RN. 2016. Investigating essential gene function in *Mycobacterium tuberculosis* using an efficient CRISPR interference system. *Nucleic Acids Res* 44:e143. <https://doi.org/10.1093/nar/gkw625>.
45. Kumar M, Khan IA, Verma V, Qazi GN. 2005. Microplate nitrate reductase assay versus Alamar Blue assay for MIC determination of *Mycobacterium tuberculosis*. *Int J Tuberc Lung Dis* 9:939–941.
46. Shin J, Baek JY, Chung DR, Ko KS. 2017. Instability of the IncFII-type plasmid carrying *bla*NDM-5 in a *Klebsiella pneumoniae* isolate. *J Microbiol Biotechnol* 27:1711–1715. <https://doi.org/10.4014/jmb.1706.06030>.